University of Zurich[UZH]

Zurich Open Repository and Archive
University of Zurich
University Library
Strickhofstrasse 39
CH-8057 Zurich
www.zora.uzh.ch

Year: 2014

Interaction effects of cell diffusion, cell density and public goods properties on the evolution of cooperation in digital microbes

Dobay, Akos ; Bagheri, Homayoun C ; Messina, Antonio ; Kümmerli, Rolf ; Rankin, Daniel J

Abstract: Microbial cooperation typically consists in the sharing of secreted metabolites (referred to as public goods) within the community. Although public goods generally promote population growth, they are also vulnerable to exploitation by cheating mutants, which no longer contribute, but still benefit from the public goods produced by others. Although previous studies have identified a number of key factors that prevent the spreading of cheaters, little is known about how these factors interact and jointly shape the evolution of microbial cooperation. Here, we address this issue by investigating the interaction effects of cell diffusion, cell density, public good diffusion and durability (factors known to individually influence costs and benefits of public goods production) on selection for cooperation. To be able to quantify these effects across a wide parameter space, we developed an individual-based simulation platform, consisting of digital cooperator and cheater bacteria inhabiting a finite two-dimensional continuous toroidal surface. Our simulations, which closely mimic microbial microcolony growth, revealed that: (i) either reduced cell diffusion (which keeps cooperators together) or reduced public good diffusion (which keeps the public goods closer to the producer) is not only essential but also sufficient for cooperation to be promoted; (ii) the sign of selection for or against cooperation can change as a function of cell density and in interaction with diffusion parameters; and (iii) increased public goods durability has opposing effects on the evolution of cooperation depending on the level of cell and public good diffusion. Our work highlights that interactions between key parameters of public goods cooperation give rise to complex fitness landscapes, a finding that calls for multifactorial approaches when studying microbial cooperation in natural systems.

DOI: https://doi.org/10.1111/jeb.12437

Posted at the Zurich Open Repository and Archive, University of Zurich
ZORA URL: https://doi.org/10.5167/uzh-106226
Journal Article
Accepted Version

Originally published at:
Dobay, Akos; Bagheri, Homayoun C; Messina, Antonio; Kümmerli, Rolf; Rankin, Daniel J (2014). Interaction effects of cell diffusion, cell density and public goods properties on the evolution of cooperation in digital microbes. Journal of Evolutionary Biology, 27(9):1869-1877.
DOI: https://doi.org/10.1111/jeb.12437

Interaction effects of cell diffusion, cell density and public goods properties on the evolution of cooperation in digital microbes

Akos Dobay[1], Homayoun C. Bagheri[1], Antonio Messina[2], Rolf Kümmerli[3,*], Daniel J. Rankin[1,*]

[1]Institute of Evolutionary Biology and Environmental Studies, Winterthurerstrasse 190, University of Zurich, CH-8057 Zurich, Switzerland.

[2]Grid Computing Competence Center, Winterthurerstrasse 190, University of Zurich, CH-8057 Zurich, Switzerland.

[3]Institute of Plant Biology, Winterthurerstrasse 190, University of Zurich, CH-8057 Zurich, Switzerland.

* contributed equally

Corresponding author: Akos Dobay

Institute of Evolutionary Biology and Environmental Studies

Winterthurerstrasse 190, CH-8057 Zurich, Switzerland

Tel. +41 44 635 66 17

Fax +41 44 635 57 11

Email: Akos.Dobay@uzh.ch

Total number of words including methods, reference & figure legends: 6,611

Keywords: micro-organisms, public goods, cooperation, diffusion, durability, agent-based modelling

Abstract

Microbial cooperation typically consists in the sharing of secreted metabolites (referred to as public goods) within the community. Although public goods generally promote population growth, they are also vulnerable to exploitation by cheating mutants, which no longer contribute, but still benefit from the public goods produced by others. While previous studies have identified a number of key factors that prevent the spreading of cheats, little is known about how these factors interact and jointly shape the evolution of microbial cooperation. Here, we address this issue by investigating the interaction effects of cell diffusion, cell density, public goods diffusion and durability (factors known to individually influence costs and benefits of public goods production) on selection for cooperation. To be able to quantify these effects across a wide parameters space, we developed an individual-based simulation platform, consisting of digital cooperator and cheater bacteria inhabiting a finite continuous two-dimensional toroidal surface. Our simulations, which closely mimic microbial micro-colony growth, revealed that: (a) either reduced cell diffusion (which keeps cooperators together) or reduced public goods diffusion (which keeps the public good closer to the producer) is essential but also sufficient for cooperation to be promoted; (b) the sign of selection for or against cooperation can change as a function of cell density and in interaction with diffusion parameters; and (c) increased public goods durability has opposing effects on the evolution of cooperation depending on the level of cell and public goods diffusion. Our work highlights that interactions among key parameters of public goods cooperation give rise to complex fitness landscapes, a finding that calls for multi-factorial approaches when studying microbial cooperation in natural systems.

Introduction

Research over the past decade has revealed that microbes exhibit a multitude of cooperative behaviours (Crespi, 2001; Velicer, 2003; West *et al.*, 2007a). Microbes form fruiting bodies (Velicer & Vos, 2009; Strassmann & Queller, 2011) and biofilms (Nadell *et al.*, 2009), communicate with each other through the release and perception of signalling molecules (Bassler & Losick, 2006), and share secreted beneficial metabolites (i.e. public goods) among community members (West *et al.*, 2007a). Public goods secretion seems to be the most prominent form of cooperation, with examples comprising the release of enzymes to digest food (Greig & Travisano, 2004; Bachmann *et al.*, 2011), chelators to scavenge essential metals (Griffin *et al.*, 2004), toxins to fight competitors (Inglis *et al.*, 2009), and biosurfactants for cooperative swarming (Xavier *et al.*, 2011).

Despite the community-level benefits that arise from sharing metabolites (Ross-Gillespie *et al.*, 2007), public goods cooperation is not straightforward to explain. This is because natural selection is predicted to favour cheating mutants, which no longer contribute to the public good, but still benefit from the cooperative acts performed by others (West *et al.*, 2006; Rankin *et al.*, 2007; Ghoul *et al.*, 2014). A wealth of research has focused on understanding the factors that promote public goods cooperation in the light of the prevalent risk of cheater exploitation. This research has demonstrated that the evolutionary success of microbial cooperation depends on many factors, including strain frequency (Gilbert *et al.*, 2007; Ross-Gillespie *et al.*, 2007; Gore *et al.*, 2009), cell density (Greig & Travisano, 2004; Ross-Gillespie *et al.*, 2009), resource availability (Brockhurst *et al.*, 2008; Kümmerli *et al.*, 2009b), cell dispersal (Chao & Levin, 1981; MacLean & Brandon, 2008; Kümmerli *et al.*, 2009a; Refardt *et al.*, 2013; Julou *et al.*, 2013), diffusion of public goods (Kümmerli *et al.*, 2009a; Le Gac & Doebeli, 2010), durability of public goods (Kümmerli & Brown, 2010), regulatory mechanisms that allow an optimal timing of public goods production (Kümmerli &

74 Brown, 2010; Xavier *et al.*, 2011; Darch *et al.*, 2012), and pleiotropic effects emerging from
75 the genetic architecture of social traits (Driscoll *et al.*, 2011; Dandekar *et al.*, 2012).

76 While this body of experimental work, as a whole, demonstrates the complexity of
77 microbial public goods cooperation, individual studies usually focussed on the impact of a
78 single factor at the time (see Brockhurst *et al.*, 2010 as an exception). Here, we aim to
79 investigate how key factors of public goods cooperation interact, thereby jointly influencing
80 microbial sociality. Because laboratory experiments usually impose constraints with regard to
81 the number of factors and parameter combinations that can simultaneously be looked at, we
82 developed an individual-based simulation platform, consisting of digital microbes growing on
83 a finite off-lattice (i.e. continuous space) two-dimensional toroidal surface with connected
84 boundaries. This platform allowed us to realistically mimic microbial cooperation in
85 microcolonies (Fig. 2, Movie S1), and thus, to conduct simulations (i.e. *in silico* experiments),
86 explicitly exploring interaction effects across a large parameter space.

87 We considered two strains of digital microbes: a public-good-producing strain
88 (henceforth cooperator) and a non-public-good-producing strain (henceforth cheat). Both
89 strains had the same basic growth rate, and could move across the surface, according a cell
90 diffusion parameter. When public goods production was enabled, cooperators produced public
91 goods with specified molecular properties (i.e. diffusion, durability) at a constant rate
92 entailing a fixed cost c per molecule. The public goods generate a fixed benefit b for any
93 individual taking up a molecule from the environment, whereby $b > c$, with the cumulative
94 effects of b and c feeding into the specific growth rate of each individual. We implemented a
95 microbial life cycle that involved a cellular growth phase followed by a discrete division
96 event (Fig. 1). Moreover, through the implementation of a density-dependent death rate, we
97 could manipulate the time needed for microcolonies to reach carrying capacity. Series of
98 growth and division ended whenever the toroidal environment was close to saturation (Fig. 2).

We used our platform to quantify the fitness of cooperators and cheats, and the sharing of public goods in the community as a function of cell diffusion and density, as well as public goods diffusion and durability. Theoretical work has revealed that both cell diffusion (determining to which degree cooperators stay together) and public goods diffusion (determining the scale over which metabolites can be shared) significantly impact the evolution of public goods cooperation (Allison, 2005; Ross-Gillespie *et al.*, 2009; Driscoll & Pepper, 2010; Allen *et al.*, 2013; Borenstein *et al.*, 2013). Here, we quantify the interaction effects between these important parameters. In addition, we assess the role of public goods durability in interaction with cell and public goods diffusion. Molecular durability is an important property of secreted molecules because it determines the time a public good remains available for both cooperators and cheats. However, its impact on the evolution of microbial cooperation is controversial because some have argued that increased durability is always beneficial for cooperation in colonies (Allen *et al.*, 2013), whereas others have shown that it can also hinder cooperation in a meta-population because cheats have access to public goods for extended periods of time, even following local cooperator extinction (Brown & Taddei, 2007; Kümmerli & Brown, 2010). Finally, we study the interaction between cell density and the diffusion properties of cells/public goods by: (a) comparing the performance of cooperators and cheats during early versus late stages of microcolony formation; and (b) varying the density-dependent death rate, which allowed us to manipulate the time microcolonies spent at high cell density. While empirical work showed that low cell density favours cooperation when public goods diffusion is reduced (Greig & Travisano, 2004; Ross-Gillespie *et al.*, 2009), its impact on the evolution of public goods cooperation under conditions where cell and/or public goods diffuse more readily are unclear.

Materials and methods

In silico bacterial habitat

We created a finite, two-dimensional continuous (off-lattice) landscape with double-precision numbers. The landscape forms a torus of 40 x 40 µm (1600 μm^2) with connected boundaries, in which bacteria were seeded and allowed to grow and divide according to specific rules (see below). All simulations were performed using an agent-based multidimensional (2D) framework.

Bacterial life cycle

At the start of each simulation, we seeded two bacteria, one public-good producer and one non-producer cell, to random locations onto the landscape. Each bacterium was implemented as a filled disk with a radius of 1 µm at the start of its life cycle. The bacteria then started growing, whereby the growth of public-good producers G_p and non-producers G_{np} is defined by the following recursive functions

$$G_p(t+1) = \left(\mu + b\sum_j p_j - c\right)G_p(t) \quad (1)$$

and

$$G_{np}(t+1) = \left(\mu + b\sum_j p_j\right)G_{np}(t) \quad (2)$$

where μ is a strictly positive number representing the growth rate. The other parameters in (1) and (2) are $\sum_j p_j$, the total number of public goods consumed, and b and c the benefit and the cost values respectively of public goods production (with $b = 0.01$ and $c = 0.001$).

Cell growth was followed by division (Fig. 1), which automatically occurred when a cell reached the threshold radius of 2 µm. Cell division created a mother and a daughter cell of equal size, such that the sum of the surface area of both mother and daughter cells equalled the surface area of the parental cell. The position of the daughter relative to its mother was

148 determined by drawing a random value between 0 and 2π. Following positioning, cells
149 resumed growth.

150 Between the discrete rounds of growth, cells were free to move in any direction on the
151 landscape, whereby diffusion was specified by the cell diffusion parameter D_c. In biological
152 terms, this parameter combines both active cell movement and passive diffusion. The
153 diffusion process followed a Gaussian random walk, with a Gaussian random number
154 generator based on the Box-Muller transforms that convert uniformly distributed random
155 numbers (Box & Muller, 1958; Thomas *et al.*, 2007).

156 Because cell diffusion and division may result in cells overlapping with each other, we
157 had to implement a spatial correction process. Specifically, we incorporated an algorithm,
158 which is applied at every step when the size of a cell is incremented according to equation (1)
159 or (2). The moves are controlled by a variable factor proportional to the distance between two
160 neighbouring cells x_i and x_j. The new position $x_i^{(new)}$ is computed as

161 $$x_i^{(new)} = x_i^{(old)} + \lambda R \left\| x_i^{(old)} - x_j \right\| \quad (3)$$

162 where λ is set empirically to 0.1 and R is a uniform random number drawn between 0 and 1.
163 The algorithm uses a pairwise comparison to remove any spatial overlap between adjacent
164 cells.

165 Finally, we implemented cell death, whereby the probability of dying of any given
166 individual was proportional to its local cell density, computed as

167 $$Pr_{die} = \begin{cases} 1 \; if \; \alpha RT \geq \rho R \\ 0 \quad \text{otherwise} \end{cases} \quad (4)$$

168 where T is the actual size of the population and ρ the local number of cells. Hence, when the
169 actual size of the population T is larger than the number of cells in a given neighbourhood of
170 perimeter r, the probability of dying for a cell is increasing. To adjust the value of T with
171 reference to the value of ρ we used the scaling parameter α. We also implemented a

controller that allows us to switch on and off equation (4) and activate cell death only when the colony achieved a given size. Typically, this size would correspond to a specific number of cells.

Cycles of growth, division and death ended when the population reached the carrying capacity K = 500. In the absence of death, K was reached after eight doublings, a number of generations that correspond to growth patterns typically observed under conditions where public goods are important for growth (Dumas & Kümmerli, 2012). With K > 500, it became increasingly time-consuming for our current computing resources to apply our spatial correction process (equation 3) to find a solution where cells do not overlap.

Public goods production and durability

Cooperator cells produced public goods at a constant rate (one molecule per second). Public goods appear as point-like particles, characterized by a specific coefficient of diffusion D_{pg}, and durability δ. The diffusion of public goods was determined by a Gaussian random walk using the Box-Muller transforms. Public goods are submitted to the same boundary conditions as cells. The consumption of public goods by cells requires a co-localization of the public good position within the surface area of a cell. Upon consumption, the public good is removed from the system. Based on these settings, the public good used in our simulations is similar to the sugars fructose and glucose made available through the catalytic action of invertase (i.e. the enzyme embedded in the cellular membrane that hydrolysis sucrose, MacLean & Brandon, 2008).

Public goods durability δ was characterized using the exponential decay function

$$e^{-\omega \Delta t/\delta} < R \quad (5)$$

with $\omega = 0.1$, defining the stiffness of the decay, and $\Delta t = (t - t_0)$. Hence, public goods are removed based on the likelihood of drawing a random number R smaller than $e^{-\omega \Delta t/\delta}$.

197 **Simulations with digital bacteria**

198 We performed two sets of simulations. In the first set, we simultaneously varied cell dispersal
199 D_c (parameter range 0.0001 – 5 μm^2/s, in steps of 0.5 μm^2/s), public goods diffusion D_{pg}
200 (0.005 – 9 μm^2/s, in steps of 1 μm^2/s) and public goods durability δ (10 – 4510 s, in steps of
201 500 s), resulting in 1100 parameter combinations. In the second set, we simultaneously varied
202 cell dispersal and public goods diffusion (as before), and death rate (parameter range 0.00005
203 – 0.04) in steps of 0.01, resulting in 550 parameter combinations. We run 500 replicates for
204 each parameters combination.

205 In all experiments, individuals had fixed strategies (i.e. either public goods producer or
206 non-producer), with no possibilities for mutations to occur (although this option is
207 implemented in the code for future studies). After each simulation, we extracted data on the
208 mean time between two cell divisions (our measure of absolute fitness), the relative frequency
209 of cooperators and cheats (our measure of relative fitness, measured every 200 seconds), and
210 the mean per capita public good uptake rate for cooperators and cheats. The mean time
211 between two cell divisions for a given simulation was calculated by averaging across cells.

212

213 ## Results and discussion

214 **Interaction between cell and public goods diffusion**

215 We found evidence for interactions between cell and public goods diffusion in shaping the
216 evolution of cooperation, as indicated by the non-parallel lines in Fig. 3. For instance, our
217 simulations revealed that increased cell and public good diffusion concomitantly selected
218 against cooperation across most of the parameter space, but not when public goods diffusion
219 was low. Here, cooperators divided more quickly and were consistently favoured regardless
220 of the extent of cell diffusion (Fig. 3a+b, Fig. S1). This pattern can be explained by the fact
221 that, with low public goods diffusion, the range across which secreted metabolite can be

222 shared is greatly reduced, which results in producers increasingly benefiting from their own
223 molecules (Kümmerli *et al.*, 2009a). Indeed, we found that the cheaters' public good uptake
224 rates were significantly reduced (Fig. 3c, Fig. S1), and the time they needed to divide greatly
225 increased (Fig. 3b, Fig. S1) with low public goods diffusion (especially when cell diffusion
226 was low, too). This shows that metabolite secretion becomes less social with lower public
227 goods diffusion. Nonetheless, our simulations revealed that, even with minimal public good
228 and cell diffusion, secreted metabolites remained accessible to cheats to some extent (Fig. 3c,
229 Fig. S1), which shows that a complete privatization of secreted metabolites is not possible in
230 our system.

231 Furthermore, we found that cooperators divided more quickly and were always
232 favoured when cell diffusion was minimal (Fig. 3a+b, Fig. S1) regardless of the degree of
233 public goods diffusion. Increased public good diffusion simply slowed down the spreading of
234 cooperation, but never changed the direction of selection even with realistically high public
235 goods diffusion rates. The cooperators' success can be explained by the observation that
236 public goods producers and cheats formed spatially separated microcolonies (see Fig. 2 for an
237 example), such that public goods were mainly shared among cooperators (i.e. clonemates)
238 within colonies, even with high public goods diffusion (Fig. 3c, Fig. S1). Thus, our
239 simulations reveal that, across a biologically realistic range of public goods diffusion rates,
240 highly limited cell diffusion is sufficient to favour cooperation. In natural settings, limited
241 dispersal is presumably common and might be induced either passively, e.g. in viscous media
242 where microbial mobility is physically constraint (Wang & Or, 2013), or actively, by the
243 microbes themselves, for example through the secretion of extracellular polymeric substances
244 (Flemming & Wingender, 2010).

245 Our finding that local sharing of public goods among clonemates favours cooperation
246 is in accordance with inclusive fitness theory (Hamilton, 1964), which predicts that altruistic

247 forms of cooperation can be selected for when the benefit (b) of cooperation preferentially
248 accrues to relatives (r, i.e. other cooperators), such that rb outweighs the cost c of
249 cooperation ($rb > c$, see Gilbert *et al.*, 2007; Chuang *et al.*, 2010; Kümmerli *et al.*, 2010 for
250 microbial examples). However, it is important to note that limited dispersal does not
251 inevitably favour cooperation, as it also increases local competition among relatives, which
252 opposes the evolution of cooperation (Taylor, 1992). One likely explanation for why local
253 competition seems to play a minor role in our experiments is that microcolonies can expand
254 (i.e. export the benefit of cooperation Fig. 2, movie S1), a factor that has been shown to
255 attenuate local competition (Lehmann *et al.*, 2006; Alizon & Taylor, 2008).

256 When cell and public goods diffusion co-varied, cooperation was only favoured with
257 very low cell and public goods diffusion. Across the remaining parameters space, cheater
258 increased in frequency (Fig. 3a, Fig. S1). Crucially, our simulations show that cheaters could
259 spread even when having lower public good uptake rates than cooperators (Fig. 3c, Fig. S1,
260 cheater generally had lower public good uptake rates, except for D_{pg} = 3). This pattern is
261 compatible with the view that a public good is usually close to its producer immediately upon
262 secretion, and only later, through diffusion, it can reach other cells (Driscoll & Pepper, 2010;
263 Julou *et al.*, 2013). Thus, our result resolves a recent debate in the literature (Zhang & Rainey,
264 2013; Kümmerli & Ross-Gillespie, 2014; Ghoul *et al.*, 2014) by showing that equal sharing of
265 a secreted metabolite is not a precondition for a trait to be considered cooperative. Instead, a
266 trait is cooperative when others than the producers themselves gain some benefit from the
267 cooperative act (West *et al.*, 2007b), regardless of the magnitude of that benefit - a condition
268 that was satisfied across our entire parameter space (Fig. 3c, Fig. S1).

269 The fitness landscape arising from cell and public goods diffusion (Fig. 3a, Fig. S1)
270 suggests that there are two principle routes by which natural selection can promote public
271 goods cooperation in environments with high potentials for diffusion (e.g. open sea water). It

can either favour: (i) behaviours that reduce bacterial dispersal, for instance, through the formation of biofilms on substrates; or (ii) secreted metabolites with extremely reduced diffusion properties. Evidence from empirical studies on marine bacteria indeed indicates that one or the other route has been taken (Martinez *et al.*, 2003; Cordero *et al.*, 2012).

Interaction between cell density and diffusion parameters

Apart from the effect that shifts in strain frequency were less pronounced during early vs. late stages of microcolony formation (because fewer cell divisions occurred), we also found that the sign of selection (for or against cooperation) can change in function of cell density (Fig 3a+d, Fig. S1); especially with minimal cell diffusion and relatively high public goods diffusion. Here, cooperation was selected against during early phases of the colony life cycle (i.e. at low cell density, Fig. 3d, Fig. S1), whereas the pattern reversed at later stages of microcolony growth (i.e. at high cell density, Fig. 3a, Fig. S1). This pattern is in line with the observation that at early stages of microcolony formation, there are only one or a few cooperators around (Fig. 2), such that most of their public goods immediately diffuse out of their reach, thereby becoming highly accessible to cheats. Only later, once larger microcolonies have formed, increased public-goods sharing within cooperator microcolonies becomes possible, giving cooperators a fitness advantage.

An opposite change in the strength of selection emerged with relatively low public goods (e.g. $D_{pg} = 1$) and relatively high cell ($D_c \geq 2$) diffusion (Fig. 3a+d, Fig. S1). In this area of our parameter space, we seemingly recover the findings by Ross-Gillespie *et al.* (2009), where cooperation is favoured at low cell density, presumably because cheats have limited access to a poorly diffusing public good. However, this initial drop in cheater frequency is then compensated at higher cell densities, when the public good becomes more abundant and more evenly mixed across cells.

When we allowed microcolonies to grow at high cell density for extended periods of time (owing to the implementation of a density-dependent death rate), we found that under conditions of high diffusion, the increase in cheater frequency became more pronounced (Fig. 4, Fig. S2). Under conditions of low diffusion, meanwhile, higher death rates had either a minor or a positive effect on the evolution of cooperation. These patterns can be explained by the fact that death rate increases the number of generations that are needed to reach carrying capacity, which gives the dominating strain more time to translate its relative fitness benefits into frequency shifts.

These results highlight that attention must be paid to temporal effects during microbial population growth, where strength and direction of selection can vary considerably over a short period of time. In practice, these temporal effects are often ignored, and competition assays are typically run for a fixed amount of time (e.g. for 24 or 48 hours). Such temporal effects have so far only been suggested to play a role across longer time-scales, through eco-evolutionary feedbacks, whereby selection for cheats lowers population density, which in turn tempers the spreading of cheats (Ross-Gillespie *et al.*, 2007; Ross-Gillespie *et al.*, 2009; Sanchez & Gore, 2013).

Interaction between public goods durability and diffusion parameters

Our simulations revealed significant interactions between public goods durability, and cell and public goods diffusion (Fig. 5, Fig. S3). Under conditions of high public goods diffusion (which generally disfavours cooperation), high public goods durability greatly dampened the selective advantage of cheats (Fig. 5, Fig. S3). Why does extended durability, in interaction with high public goods diffusion, reduce cheater fitness? To answer that question, let us consider how the net benefits (for cooperators: $b\Sigma_j p_j - c$, for cheats $b\Sigma_j p_j$, see equations 1+2) of public goods production/uptake alters in function of durability. Because cooperators

produce public goods at a constant rate, variation in durability does not alter the production costs *c*. However, extended durability augments $b\Sigma_j p_j$ because it increases the time molecules stay in the environment, thereby increasing public goods availability and uptake rates ($\Sigma_j p_j$). Consequently, the net benefit for cooperators and cheats tend to converge with more durable public goods, thereby giving cheats less of an advantage. Important to note is that in natural systems, durability might feed back on *c*. For instance, public goods are often facultatively expressed in response to their need, which enables microbes to down-scale their investment when public goods are more durable (Kümmerli & Brown, 2010) – a regulatory response that is expected to further converge the net benefits of the two competing strains.

Under conditions of low cell and public goods diffusion, meanwhile, extended durability had either a minor or even a negative effect on the selection for cooperation (Fig. 5, Fig. S3). For instance, when $D_c = D_{pg} = 1$, the increase in the frequency of cooperators is much more pronounced with low (from 0.5 to 0.75) than high (from 0.5 to 0.64) public goods durability. This pattern can be explained by the fact that cooperators and cheats form distinct microcolonies with low cell diffusion, whereby neighbouring cells touch each other, and can therefore exchange the public goods immediately upon secretion (e.g. see Julou *et al.*, 2013). Because of this immediate exchange, extended durability is disadvantageous as it results in an increased fraction of public-good molecules leaking out of the cooperator microcolony, eventually reaching cheats.

Conclusions

Our simulations based on digital microbes proved useful in disentangling the complex interactions between key components of microbial public goods cooperation, such as cell diffusion, density and mortality, as well as public goods diffusion and durability. We recovered complex fitness landscapes and changes in the direction of selection across our

parameter space. These findings demonstrate that the effect of a single factor on the evolution of microbial public goods cooperation can only be interpreted correctly in the context of these interaction effects. For instance, the predominant view that high public goods diffusion is detrimental for the maintenance of public goods cooperation (Allison, 2005; Driscoll & Pepper, 2010; Allen *et al.*, 2013; Borenstein *et al.*, 2013) holds only for some areas of our parameter space (Fig. 3a), but not for conditions where cell diffusion was minimal. Here, cooperation was favoured (although at a lower rate) even when public goods diffusion was relatively high. Taken together, our simulations reveal that previously identified key factors of cooperation interact and thereby jointly shape the evolution of social interactions in microbes – an insight that will hopefully spur future experimental work in real microbial systems.

More generally, the simulation framework developed in this study, which realistically mimics microbial growth under conditions as occurring in well-shaken test tubes (i.e. with high cell and public good diffusion), as well as agar plates and single-layer biofilms (i.e. with reduced cell diffusion, Fig. 2), is expandable, and can be used in the future to elucidate further important aspects of microbial public goods cooperation. For example, there is the possibility to manipulate nutrient supply (Brockhurst *et al.*, 2008), and strain frequency *(*Ross-Gillespie *et al.*, 2007), two other important aspects influencing microbial public goods cooperation, as well as allowing mutations to arise to simulate experimental evolution (Harrison *et al.*, 2008; Dumas & Kümmerli, 2012). Moreover, it would be interesting to see how the mode of action of a public good affects evolutionary dynamics of cooperation. While we simulated a public good that can generate immediate benefits (analogous to the sugars made publically available through the catalytic action of the membrane-bound invertase in yeast Greig & Travisano, 2004), other secreted metabolites, such as siderophores (to bind iron; Griffin *et al.*, 2004) and proteases (to digest tissue; Diggle *et al.*, 2007) must first diffuse away from the cell to engage in a chemical reaction with a substrate before they can generate benefits.

372

373 Acknowledgments

374 This work was supported by the Swiss National Science Foundation Grants 31003A-125457
375 (to DR) and PP00P3-139164 (to RK), and the canton of Zurich (to HB). AD thanks the
376 support group of the SGI Altix UV system, called Hydra (www.scicomp.uzh.ch/hydra.html),
377 at the computing facility of the university of Zurich for maintaining the computing resources
378 required in the framework of this project and the Grid Computing Competence Center of the
379 University of Zurich (http://www.gc3.uzh.ch) for maintaining the computing resources on the
380 cloud infrastructure called Hobbes (http://www.gc3.uzh.ch/infrastructure/hobbes). AD and
381 DR thank Andreas Wagner for providing office space and computer facilities at the university
382 of Zurich during their stay in his research group.

383

Figure Legends

Figure 1. Flowchart depicting the numerical process by which each digital cell grows and divides on a continuous (off-lattice) surface. The horizontal arrow indicates spatial growth (from A to B and from C to D), while the vertical arrow indicates successive division events (from A to C and from C to E). During individual growth, the radius of the disk is increased until it reaches a specific length. At each division, two new disks, whose total surface equals the original one (not shown in the figure), replace the original disk. The position of the two new disks is placed along an axis randomly oriented between 0 and 2π.

Figure 2. Snapshots of a typical simulation showing microcolony growth of cooperators (green disks) and cheats (purple disks) with $D_c = 0.0005$, $D_{pg} = 5$, $\delta = 510$, $\tau = 0.0005$. *N* and *C* indicate the total number of cells and the proportion of cooperators, respectively.

Figure 3. Plots depicting (a) the relative frequency of cooperators at carrying capacity $K = 500$, (b) the mean time needed for cooperators (solid lines) and cheats (dash-dotted lines) to divide, and (c) the mean public good uptake rates of the two strains, as a function of cell diffusion (varying along the x-axis) and public goods diffusion (varying from low to high following the indicated heat map). (d) Plot showing the relative frequency of cooperators after 1/3 of the time needed to reach carrying capacity *K*. Mean values have been calculated on the basis of 500 independent runs. Error bars correspond to the standard error of the mean. They are about the size of the lines connecting the data points. Public goods durability and death rate were kept constant at $\delta = 510$, $\tau = 0.00005$.

Figure 4. Relative cooperator frequency at carrying $K = 500$, as a function of cell diffusion (varying along the x-axis), public goods diffusion (varying from low to high following the

indicated heat map), and death rate (τ = 0.00005 for dash-dotted lines; τ = 0.04 for solid lines). Mean values have been calculated on the basis of 500 independent runs. Error bars correspond to the standard error of the mean. They are about the size of the lines connecting the data points. Public goods durability was kept constant at δ = 510.

Figure 5. Plot of the relative cooperator frequency at carrying K = 500, as a function of cell diffusion (varying along the x-axis), public goods diffusion (varying from low to high following the indicated heat map), and public goods durability (δ = 10 for dash-dotted lines; δ = 4510 for solid lines). Mean values have been calculated on the basis of 500 independent runs. Error bars correspond to the standard error of the mean. They are about the size of the lines connecting the data points. Death rate was kept constant at τ = 0.00005.

Supplementary Information

Figure S1. Landscapes depicting (a) the relative frequency of cooperators, (b) the absolute fitness of cooperators (green) and cheats (purple), and (c) the mean public good uptake rates of the two strains as a function of cell and public goods diffusion. In (a), the blue dots and the blue interpolated surface show cooperator frequency during the early stages of microcolony formation (i.e. after 1/3 of the time needed to reach carrying capacity K), whereas the red dots and surface depict cooperator frequency at K = 500. Mean values have been calculated on the basis of 500 independent runs and are depicted by dots. Error bars correspond to the standard error of the mean. They are about the size of the data points. Public goods durability and death rate were kept constant at δ = 510, τ = 0.00005.

Figure S2. Landscape of the relative cooperator frequency at carrying K = 500 as a function of cell diffusion, public goods diffusion and death rate (τ = 0 for blue dots and surface; τ =

0.04 for red dots and surface). Mean values have been calculated on the basis of 500 independent runs. Error bars correspond to the standard error of the mean. They are about the size of the data points. Public goods durability was kept constant at $\delta = 510$.

Figure S3. Landscape of the relative cooperator frequency at carrying $K = 500$ as a function of cell diffusion, public goods diffusion and public goods durability ($\delta = 10$ for blue dots and surface; $\delta = 4510$ for red dots and surface). Mean values have been calculated on the basis of 500 independent runs. Error bars correspond to the standard error of the mean. They are about the size of the data points. Death rate was kept constant at $\tau = 0.00005$.

Movie S1. A computer animation visualizing micro-colony growth in a mixed population of cooperators (green disks) and cheats (purple disks). The animation shows that cheats divide more quickly during the initial growth phase because they have unrestricted access to the highly diffusible public good (white dots). This pattern reverses at later growth stages, where cooperators and cheats form distinct clusters, such that most of the public good is shared among cooperators, giving them a significant fitness advantage. Parameter values: $D_c = 0.0005$, $D_{pg} = 5$, $\delta = 510$, $\tau = 0.0005$.

References

Alizon, S. & Taylor, P. 2008. Empty sites can promote altruistic behavior. *Evolution* **62**: 1335-1344.

Allen, B., Gore, J. & Nowak, M. A. 2013. Spatial dilemmas of diffusible public goods. *eLife* **2**: e01169.

Allison, S. D. 2005. Cheaters, diffusion and nutrients constrain decomposition by microbial enzymes in spatially structured environments. *Ecol. Lett.* **8**: 626-635.

Bachmann, H., Molenaar, D., Kleerebezem, M. & van Hylckama Vlieg, J. E. T. 2011. High local substrate availability stabilizes a cooperative trait. *ISME J.* **5**: 929-932.

Bassler, B. L. & Losick, R. 2006. Bacterially speaking. *Cell* **125**: 237-246.

Borenstein, D. B., Meir, Y., Shaevitz, J. W. & Wingreen, N. S. 2013. Non-local interaction via diffusible resource prevents coexistence of cooperators and cheaters in a lattice model. *PLoS One* **8**: e63304.

Box, G. E. P. & Muller, M. E. 1958. A note on the generation of random normal deviates. *Ann. Math. Stat.* **29**: 610-611.

Brockhurst, M. A., Buckling, A., Racey, D. & Gardner, A. 2008. Resource supply and the evolution of public-goods cooperation in bacteria. *BMC Biol.* **6**: 20.

Brockhurst, M. A., Habets, M. G. J. L., Libberton, B., Buckling, A. & Gardner, A. 2010. Ecological drivers of the evolution of public-goods cooperation in bacteria. *Ecology* **91**: 334-340.

Brown, S. P. & Taddei, F. 2007. The durability of public goods changes the dynamics and nature of social dilemmas. *PLoS One* **2**: e593.

Chao, L. & Levin, B. R. 1981. Structured habitats and the evolution of anticompetitor toxins in bacteria. *Proc. Natl. Acad. Sci. U.S.A.* **78**: 6324-6328.

Chuang, J. S., Rivoire, O. & Leibler, S. 2010. Cooperation and Hamilton's rule in a simple synthetic microbial system. *Mol. Syst. Biol.* **6**: 398.

Cordero, O. X., Ventouras, L.-A., DeLong, E. F. & Polz, M. F. 2012. Public good dynamics drive evolution of iron acquisition strategies in natural bacterioplankton populations. *Proc. Natl. Acad. Sci. U.S.A.* **109**: 20059-20064.

Crespi, B. J. 2001. The evolution of social behavior in microorganisms. *Trends Ecol. Evol.* **16**: 178-183.

Dandekar, A. A., Chugani, S. & Greenberg, E. P. 2012. Bacterial quorum sensing and metabolic incentives to cooperate. *Science* **338**: 264-266.

Darch, S. E., West, S. A., Winzer, K. & Diggle, S. P. 2012. Density-dependent fitness benefits in quorum-sensing bacterial populations. *Proc. Natl. Acad. Sci. U.S.A.* **109**: 8259-8263.

Diggle, S. P., Griffin, A. S., Campell, G. S. & West, S. A. 2007. Cooperation and conflict in quorum-sensing bacterial populations. *Nature* **450**: 411-414.

Driscoll, W. W. & Pepper, J. W. 2010. Theory for the evolution of diffusible external goods. *Evolution* **64**: 2682-2687.

Driscoll, W. W., Pepper, J. W., Pierson, L. S. & Pierson, E. A. 2011. Spontaneous Gac mutants of *Pseudomonas* biological control strains: cheaters or mutualists. *Appl. Environ. Microbiol.* **77**: 7227-7235.

Dumas, Z. & Kümmerli, R. 2012. Cost of cooperation rules selection for cheats in bacterial metapopulations. *J. Evol. Biol.* **25**: 473-484.

Flemming, H.-C. & Wingender, J. 2010. The biofilm matrix. *Nat. Rev. Microbiol.* **8**: 623-633.

Ghoul, M., Griffin, A. S. & West, S. A. 2014. Towards and evolutionary definition of cheating. *Evolution* **68**: 318-331.

Gilbert, O. M., Foster, K. R., Mehdiabadi, N. J., Strassmann, J. E. & Queller, D. C. 2007. High relatedness maintains multicellular cooperation in a social amoeba by controlling cheater mutants. *Proc. Natl. Acad. Sci. U.S.A.* **104**: 8913-8917.

Gore, J., Youk, H. & van Oudenaarden, A. 2009. Snowdrift game dynamics and facultative cheating in yeast. *Nature* **456**: 253-256.

Greig, D. & Travisano, M. 2004. The Prisoner's Dilemma and polymorphism in yeast *SUC* genes. *Biol. Lett.* **Supplements 3**: S25-S26.

Griffin, A., West, S. A. & Buckling, A. 2004. Cooperation and competition in pathogenic bacteria. *Nature* **430**: 1024-1027.

Hamilton, W. D. 1964. The genetical evolution of social behaviour I. *J. Theor. Biol.* **7**: 1-16.

Harrison, F., Paul, J., Massey, R. C. & Buckling, A. 2008. Interspecific competition and siderophore-mediated cooperation in *Pseudomonas aeruginosa*. *ISME J.* **2**: 49-55.

Inglis, R. F., Gardner, A., Cornelis, P. & Buckling, A. 2009. Spite and virulence in the bacterium *Pseudomonas aeruginosa*. *Proc. Natl. Acad. Sci. U.S.A.* **106**: 5703-5707.

Julou, T., Mora, T., Guillon, L., Croquette, V., Schalk, I. J., Bensimon, D. & Desprat, N. 2013. Cell-cell contacts confine public goods diffusion inside *Pseudomonas aeruginosa* clonal microcolonies. *Proc. Natl. Acad. Sci. U.S.A.* **110**: 12577-12582.

Kümmerli, R. & Brown, S. P. 2010. Molecular and regulatory properties of a public good shape the evolution of cooperation. *Proc. Natl. Acad. Sci. U.S.A.* **107**: 18921-18926.

Kümmerli, R., Griffin, A. S., West, S. A., Buckling, A. & Harrison, F. 2009a. Viscous medium promotes cooperation in the pathogenic bacterium *Pseudomonas aeruginosa*. *Proc. R. Soc. B* **276**: 3531-3538.

Kümmerli, R., Jiricny, N., Clarke, L. S., West, S. A. & Griffin, A. S. 2009b. Phenotypic plasticity of a cooperative behaviour in bacteria. *J. Evol. Biol.* **22**: 589-598.

Kümmerli, R. & Ross-Gillespie, A. 2014. Explaining the sociobiology of pyoverdin producing *Pseudomonas* - a comment on Zhang & Rainey (2013). *Evolution*.

Kümmerli, R., van den Berg, P., Griffin, A. S., West, S. A. & Gardner, A. 2010. Repression of competition promotes cooperation: experimental evidence from bacteria. *J. Evol. Biol.* **23**: 699-706.

Le Gac, M. & Doebeli, M. 2010. Environmental viscosity does not affect the evolution of cooperation during experimental evolution of colicigenic bacteria. *Evolution* **64**: 522-533.

Lehmann, L., Perrin, N. & Rousset, F. 2006. Population demography and the evolution of helping behaviors. *Evolution* **60**: 1137-1151.

MacLean, R. C. & Brandon, C. 2008. Stable public goods cooperation and dynamic social interactions in yeast. *J. Evol. Biol.* **21**: 1836-1843.

Martinez, J. L., Carter-Franklin, J. N., Mann, E. L., Martin, J. D., Haygood, M. G. & Butler, A. 2003. Structure and membrane affinity of a suite of amphiphilic siderophores produced by a marine bacterium. *Proc. Natl. Acad. Sci. U.S.A.* **100**: 3754-3759.

Nadell, C. D., Xavier, J. B. & Foster, K. R. 2009. The sociobiology of biofilms. *FEMS Microbiol. Rev.* **33**: 206-224.

Rankin, D. J., Bargum, K. & Kokko, H. 2007. The tragedy of the commons in evolutionary biology. *Trends Ecol. Evol.* **22**: 643-651.

Refardt, D., Bergmiller, T. & Kümmerli, R. 2013. Altruism can evolve when relatedness is low: evidence from bacteria committing suicide upon phage infection. *Proc. R. Soc. B* **280**: 20123035.

Ross-Gillespie, A., Gardner, A., Buckling, A., West, S. A. & Griffin, A. S. 2009. Density dependence and cooperation: theory and a test with bacteria. *Evolution* **63**: 2315-2325.

Ross-Gillespie, A., Gardner, A., West, S. A. & Griffin, A. S. 2007. Frequency dependence and cooperation: theory and a test with bacteria. *Am. Nat.* **170**: 331-342.

Sanchez, A. & Gore, J. 2013. Feedback between population and evolutionary dynamics determines the fate of social microbial populations. *PLoS Biology* **11**: e1001547.

Strassmann, J. E. & Queller, D. C. 2011. Evolution of cooperation and control of cheating in a social microbe. *Proc. Natl. Acad. Sci. U.S.A.* **108**: 10855-10862.

Taylor, P. D. 1992. Altruism in viscous populations - an inclusive fitness model. *Evol. Ecol.* **6**: 352-356.

Thomas, D. B., Luk, W., Leong, P. H. W. & Villasenor, J. D. 2007. Gaussian random number generators. *ACM Comput. Serv.* **39**: 11.

Velicer, G. J. 2003. Social strife in the microbial world. *Trends Microbiol.* **11**: 330-337.

Velicer, G. J. & Vos, M. 2009. Sociobiology of the *Myxobacteria*. *Annu. Rev. Microbiol.* **63**: 599-623.

Wang, G. & Or, D. 2013. Hydration dynamics promote bacterial coexistence on rough surfaces. *ISME J.* **7**: 395-404.

West, S. A., Diggle, S. P., Buckling, A., Gardner, A. & Griffin, A. S. 2007a. The social lives of microbes. *Annu. Rev. Ecol. Evol. Syst.* **38**: 53-77.

West, S. A., Griffin, A. S. & Gardner, A. 2007b. Social semantics: altruism, cooperation, mutualism, strong reciprocity and group selection. *J. Evol. Biol.* **20**: 415-432.

West, S. A., Griffin, A. S., Gardner, A. & Diggle, S. P. 2006. Social evolution theory for microorganisms. *Nat. Rev. Microbiol.* **4**: 597-607.

Xavier, J. B., Kim, W. & Foster, K. R. 2011. A molecular mechanism that stabilizes cooperative secretions in *Pseudomonas aeruginosa*. *Mol. Microbiol.* **79**: 166-179.

Zhang, X. X. & Rainey, P. B. 2013. Exploring the sociobiology of pyoverdin-producing *Pseudomonas*. *Evolution* **67**: 3161-3174.

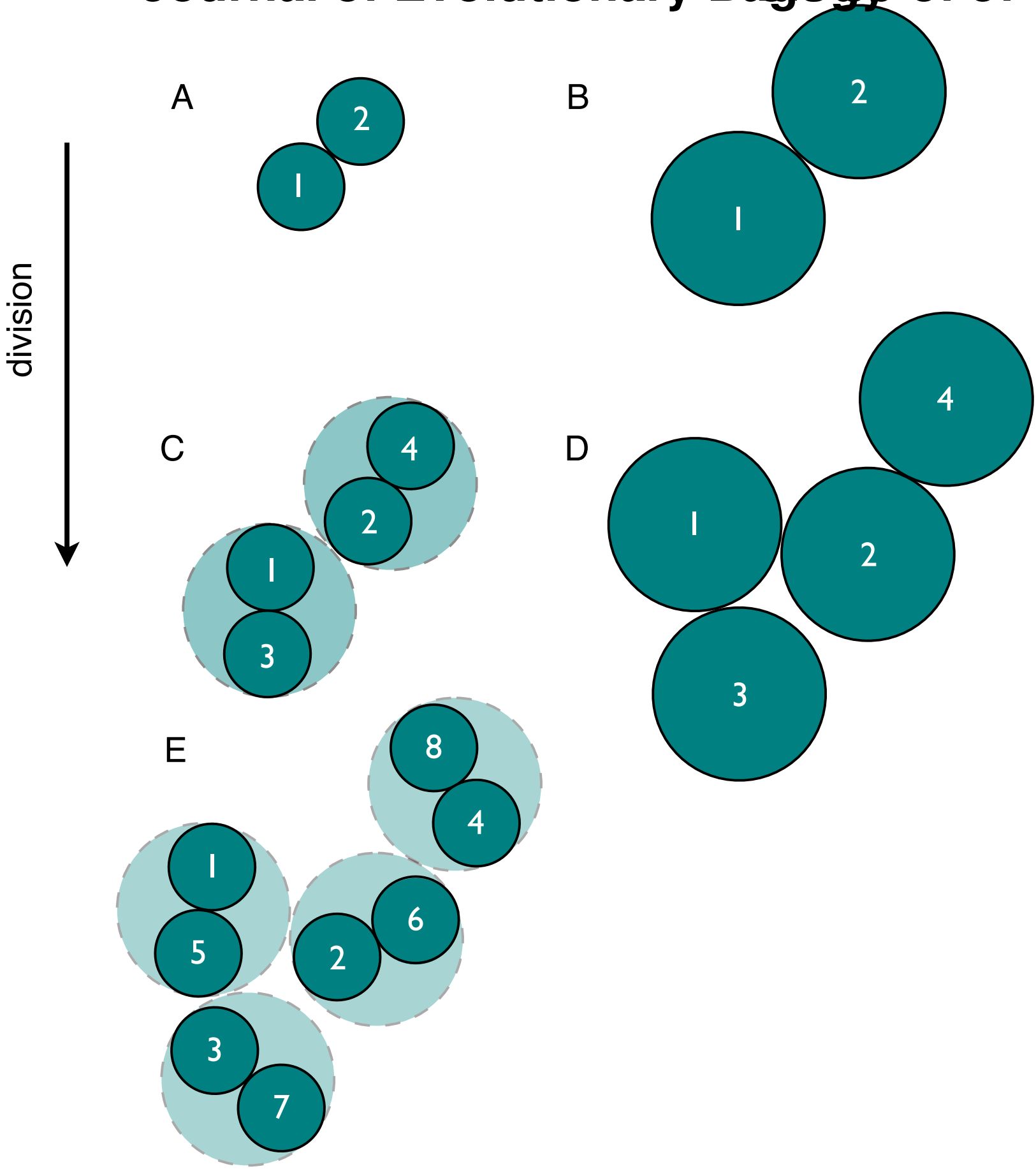
growth
division
A
2
1
B
2
1
C
4
2
1
3
D
4
1
2
3
E
8
4
1
5
6
2
3
7

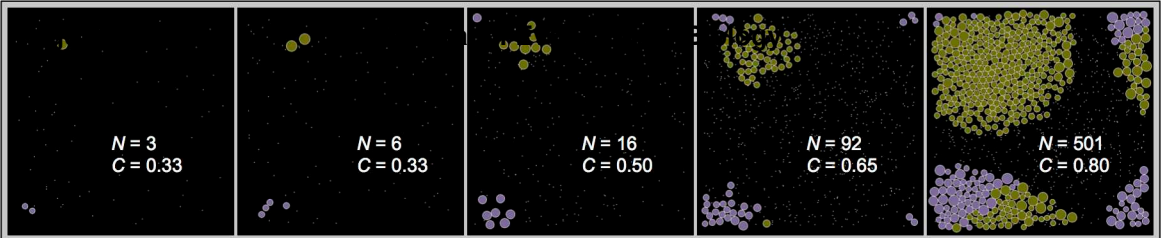
N = 3
C = 0.33
N = 6
C = 0.33
N = 16
C = 0.50
N = 92
C = 0.65
N = 501
C = 0.80
16 min
32 min
48 min
64 min
80 min

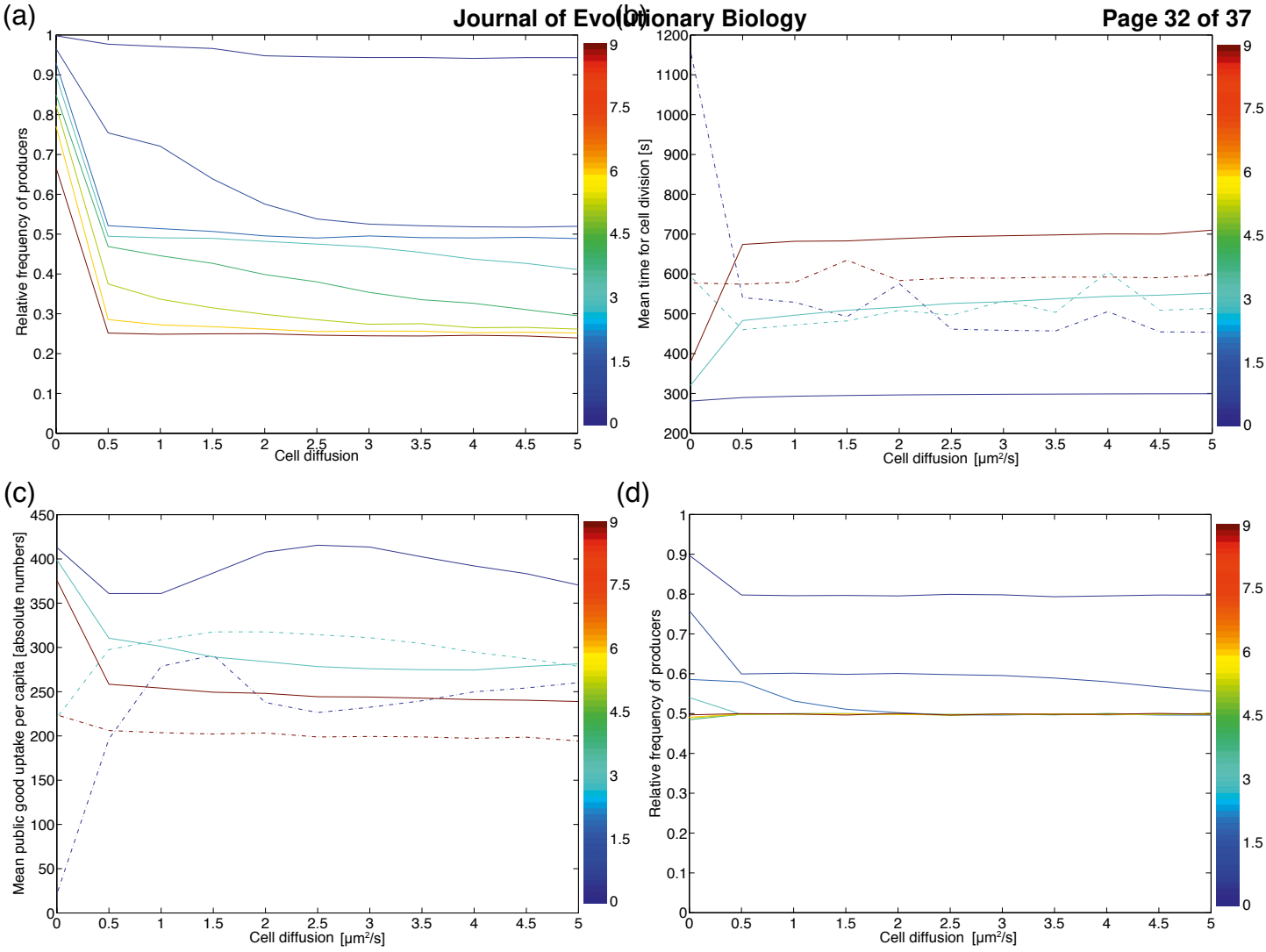
(a)
Relative frequency of producers
Cell diffusion
(b)
Mean time for cell division [s]
Cell diffusion [μm²/s]
(c)
Mean public good uptake per capita [absolute numbers]
Cell diffusion [μm²/s]
(d)
Relative frequency of producers
Cell diffusion [μm²/s]

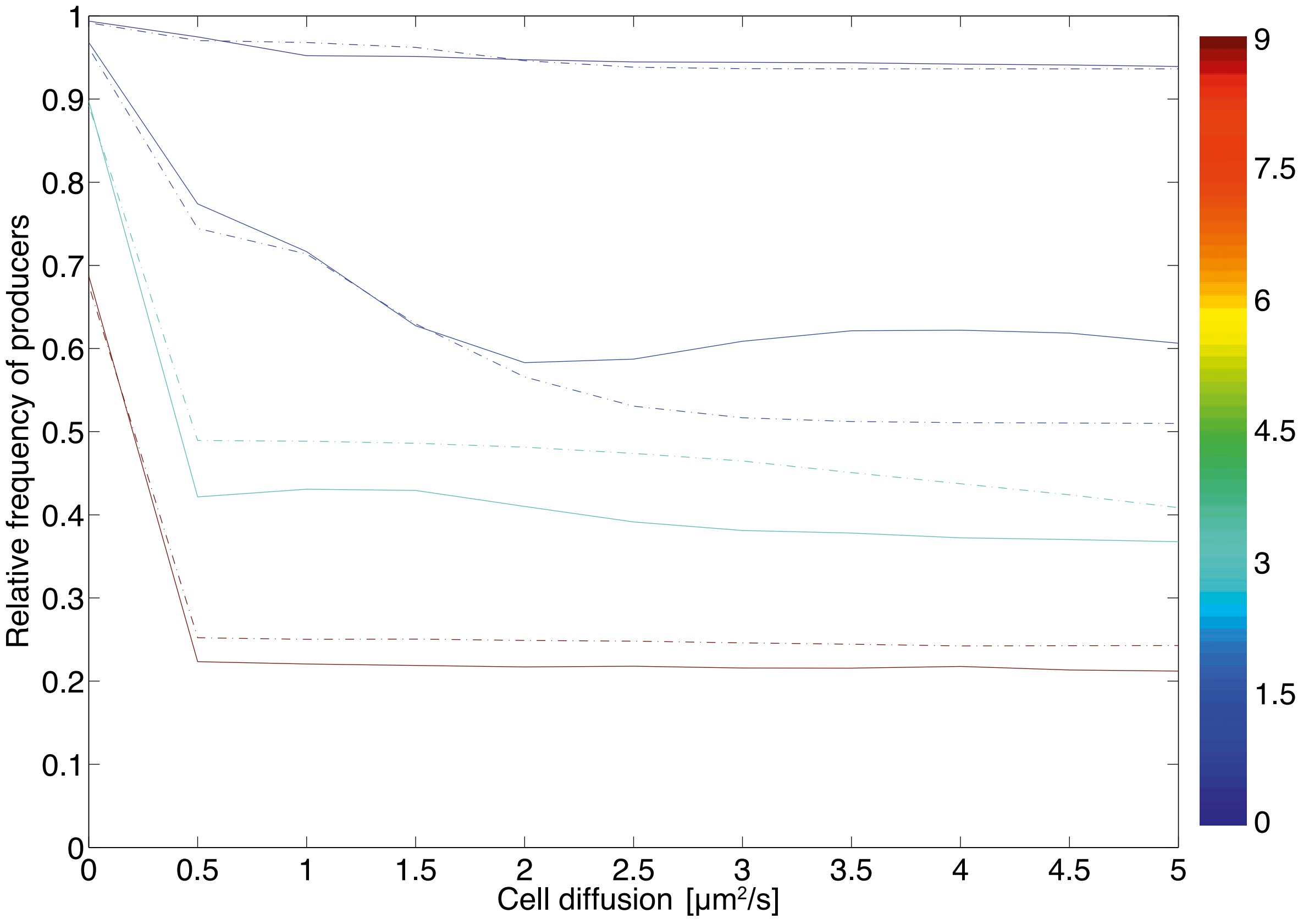
Relative frequency of producers
Cell diffusion [μm²/s]
0
0.1
0.2
0.3
0.4
0.5
0.6
0.7
0.8
0.9
1
0
0.5
1
1.5
2
2.5
3
3.5
4
4.5
5
9
7.5
6
4.5
3
1.5
0

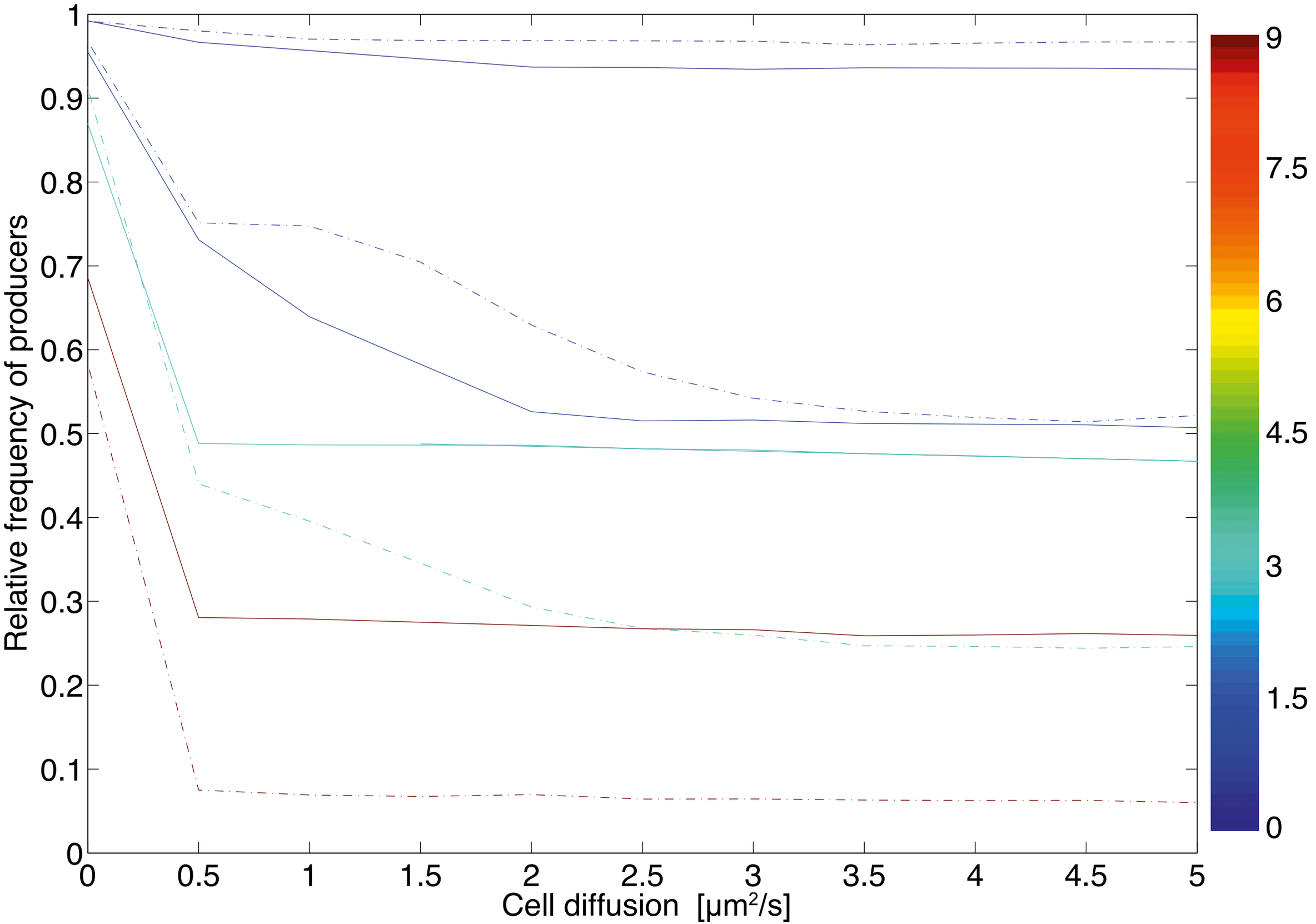
Relative frequency of producers
1
0.9
0.8
0.7
0.6
0.5
0.4
0.3
0.2
0.1
0
0
0.5
1
1.5
2
2.5
3
3.5
4
4.5
5
Cell diffusion [μm²/s]
9
7.5
6
4.5
3
1.5
0

(a)

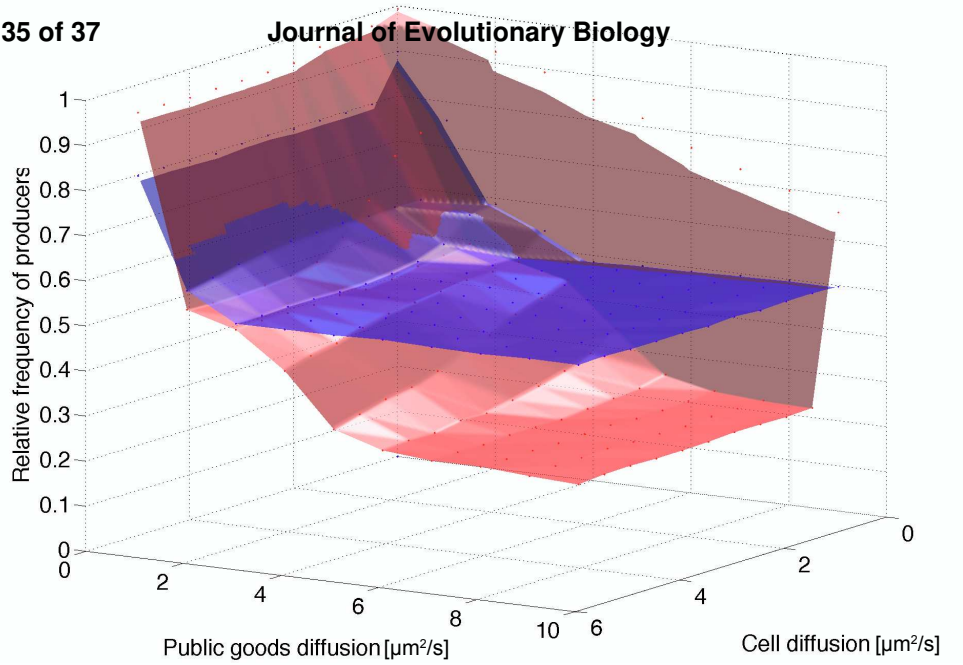
Relative frequency of producers
1
0.9
0.8
0.7
0.6
0.5
0.4
0.3
0.2
0.1
0
0
2
4
6
8
10
Public goods diffusion [μm²/s]
6
4
2
0
Cell diffusion [μm²/s]

(b)

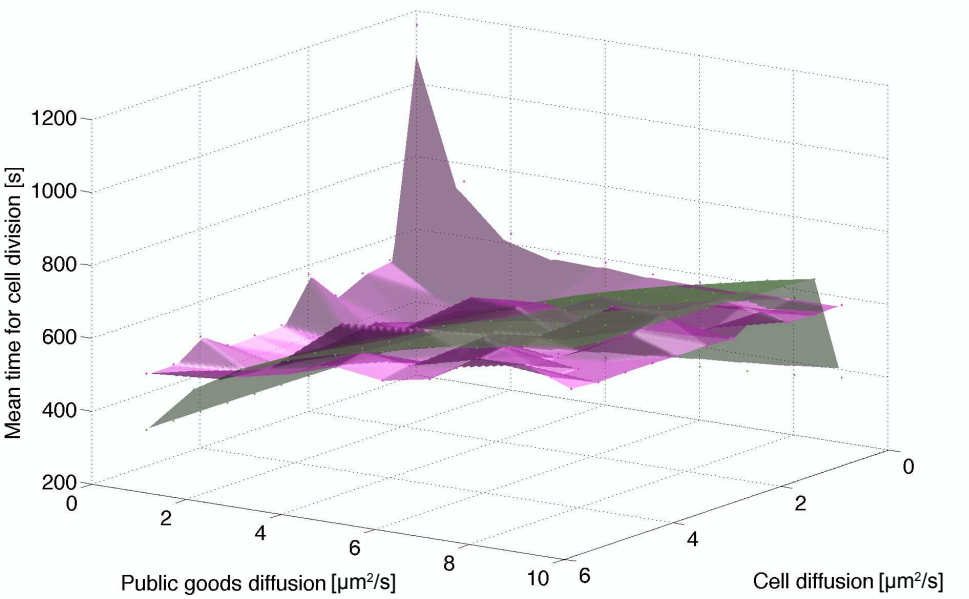
Mean time for cell division [s]
1200
1000
800
600
400
200
0
2
4
6
8
10
Public goods diffusion [μm²/s]
6
4
2
0
Cell diffusion [μm²/s]

(c)

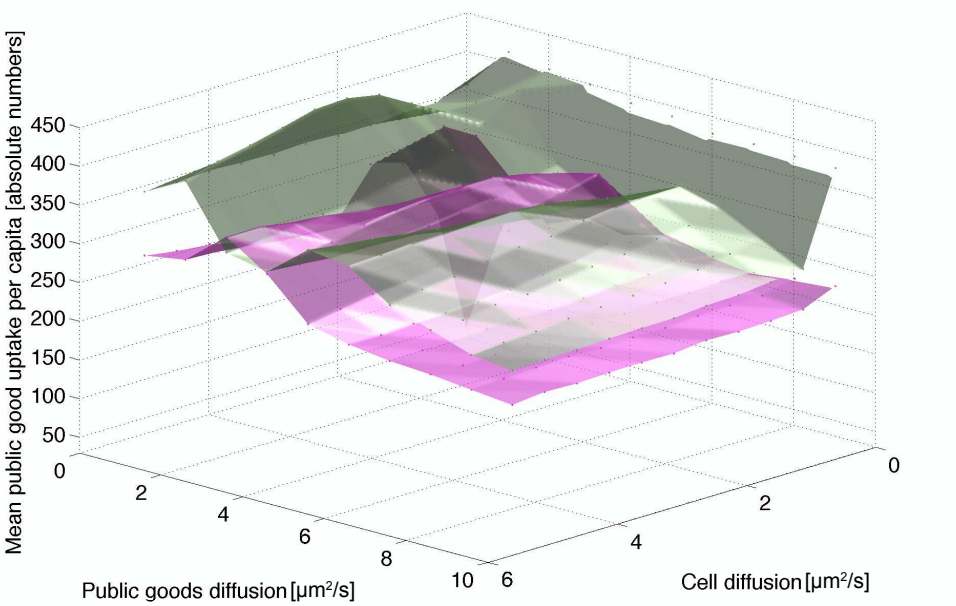
Mean public good uptake per capita [absolute numbers]
450
400
350
300
250
200
150
100
50
0
2
4
6
8
10
Public goods diffusion [μm²/s]
6
4
2
0
Cell diffusion [μm²/s]

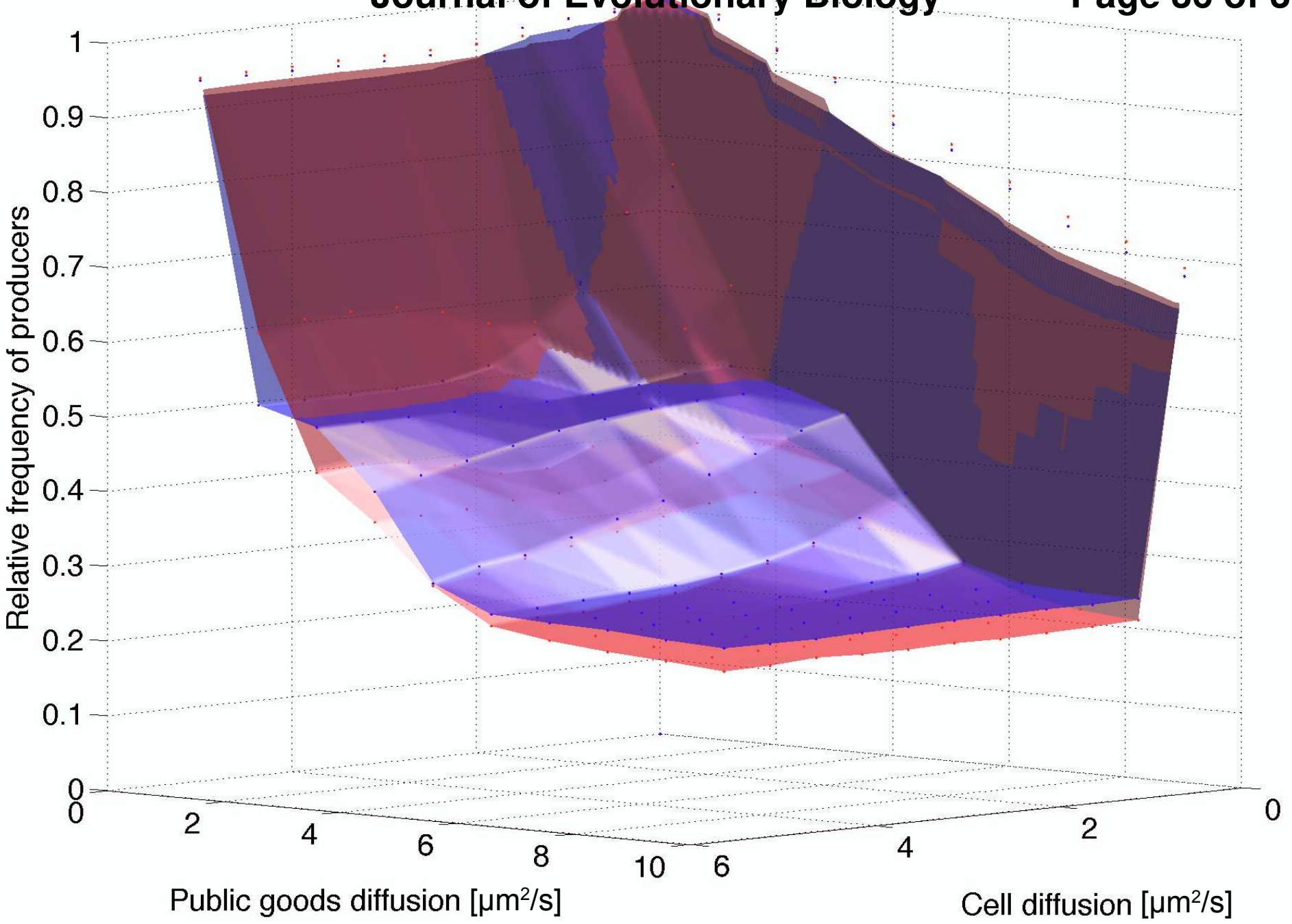
Relative frequency of producers
1
0.9
0.8
0.7
0.6
0.5
0.4
0.3
0.2
0.1
0
0
2
4
6
8
10
Public goods diffusion [μm²/s]
6
4
2
0
Cell diffusion [μm²/s]

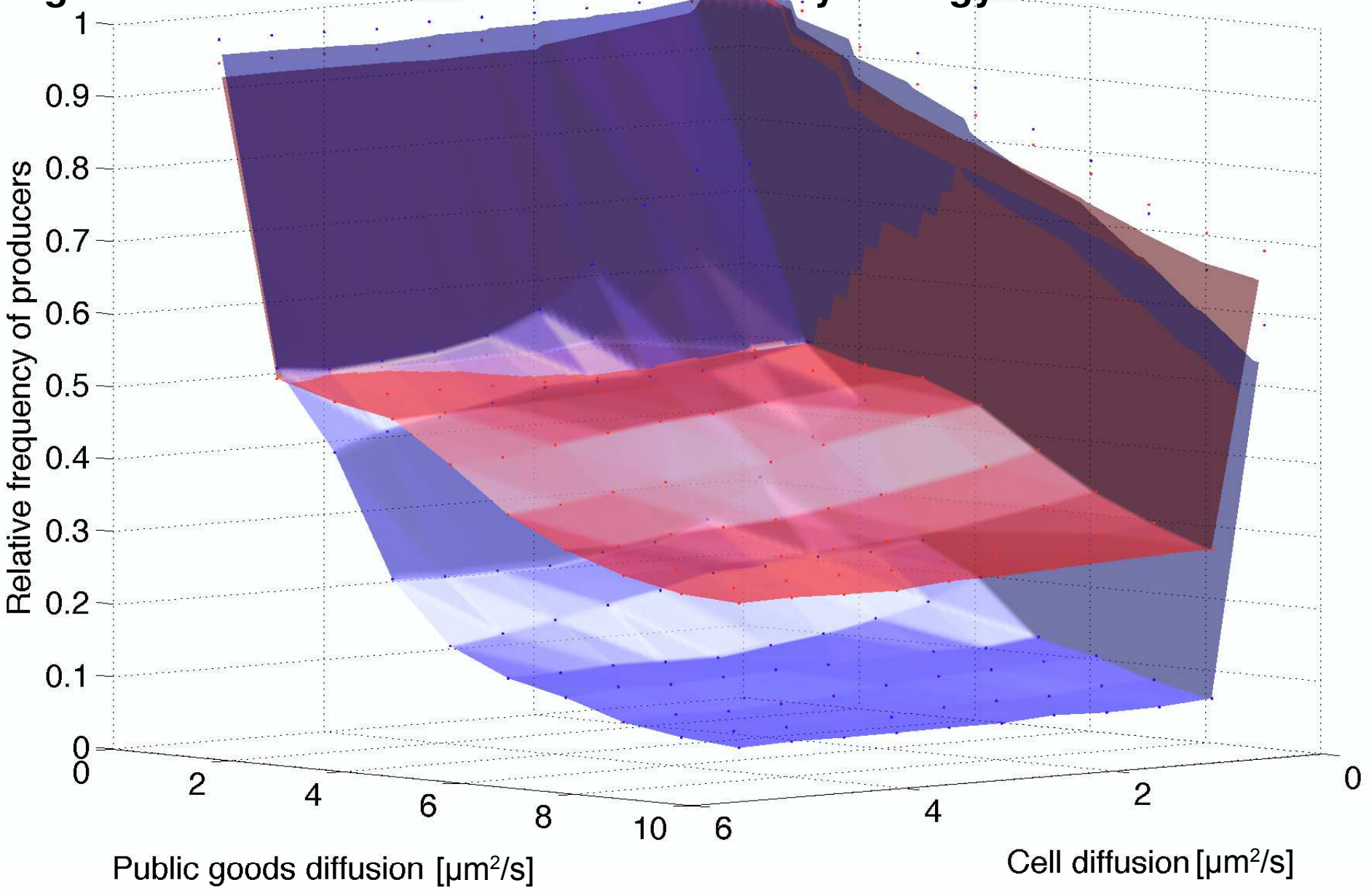
Relative frequency of producers
1
0.9
0.8
0.7
0.6
0.5
0.4
0.3
0.2
0.1
0
0
2
4
6
8
10
Public goods diffusion [μm²/s]
6
4
2
0
Cell diffusion [μm²/s]